ACS Catalysis

Letter

pubs.acs.org/acscatalysis

Photocatalytic H_2O_2 Production from Ethanol/O_2 System Using TiO_2 Loaded with Au–Ag Bimetallic Alloy Nanoparticles

Daijiro Tsukamoto,[†] Akimitsu Shiro,[†] Yasuhiro Shiraishi,*[,†] Yoshitsune Sugano,[†] Satoshi Ichikawa,[‡] Shunsuke Tanaka,[§] and Takayuki Hirai[†]

[†]Research Center for Solar Energy Chemistry, and Division of Chemical Engineering, Graduate School of Engineering Science, Osaka University, Toyonaka 560-8531, Japan

[‡]Institute for NanoScience Design, Osaka University, Toyonaka 560-8531, Japan

[§]Department of Chemical, Energy and Environmental Engineering, Kansai University, Suita 564-8680, Japan

Supporting Information

ABSTRACT: TiO_2 loaded with Au–Ag bimetallic alloy particles efficiently produces H_2O_2 from an O_2-saturated ethanol/water mixture under UV irradiation. This is achieved via the double effects created by the alloy particles. One is the efficient photocatalytic reduction of O_2 on the Au atoms promoting enhanced H_2O_2 formation, due to the efficient separation of photoformed electron–hole pairs at the alloy/TiO_2 heterojunction. Second is the suppressed photocatalytic decomposition of formed H_2O_2 due to the decreased adsorption of H_2O_2 onto the Au atoms.

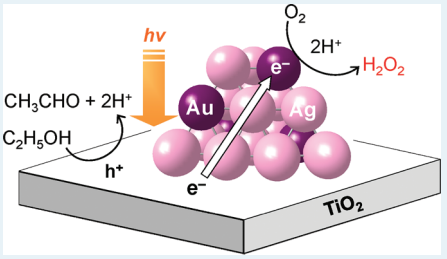

KEYWORDS: *photocatalysis, titanium dioxide, nanoparticle, alloy, hydrogen peroxide*

Hydrogen peroxide (H_2O_2) is a clean oxidant that emits only water as a byproduct and is widely used in industry for organic synthesis, pulp bleaching, wastewater treatment, and disinfection.[1] At present, H_2O_2 is commercially produced by the anthraquinone method, but the process has some nongreen features such as high energy utilization because of the multistep hydrogenation and oxidation reactions. Recently, H_2O_2 production from H_2 and O_2 gases has been studied extensively with Pd or Au–Pd bimetallic catalysts.[2−7] This direct synthesis is considered to be an alternative process from the viewpoint of green chemistry, although some care is required for operation because of the potentially explosive nature of H_2/O_2 mixtures.[8]

Photocatalytic H_2O_2 synthesis with semiconductor titanium dioxide (TiO_2) has also attracted much attention.[9−12] The reaction is usually carried out by UV irradiation of an O_2-saturated water with catalyst in the presence of electron donor such as alcohols.[9] As shown in Scheme 1a, photoexcitation of TiO_2 produces the electron (e^-) and positive hole (h^+) pairs. H_2O_2 is formed by two-electron reduction of O_2 ($O_2 + 2H^+ + 2e^- \rightarrow H_2O_2$). The reaction proceeds at room temperature without H_2 gas and can be a clean and safe H_2O_2 synthesis. The amount of H_2O_2 produced is, however, significantly low (<0.2 mM). This is because the formed H_2O_2 is converted to the peroxy species (Ti–OOH) via the reaction with surface Ti–OH groups and decomposed by the reduction with e^- (Ti–OOH + H^+ + $e^- \rightarrow$ Ti–OH + OH^-).[10] Maurino et al.[11] reported that a surface-fluorination of TiO_2 by hydrofluoric acid suppresses the formation of Ti–OOH species and produces H_2O_2 at a millimolar level; however, the resulting solution is contaminated with a large amount of fluoride.

The cleanest and the most efficient system for photocatalytic H_2O_2 synthesis is TiO_2 loaded with Au particles (Au/TiO_2).[12]

Scheme 1. Photocatalytic Formation and Decomposition of H_2O_2 on (a) TiO_2 and (b) Au/TiO_2 Catalysts

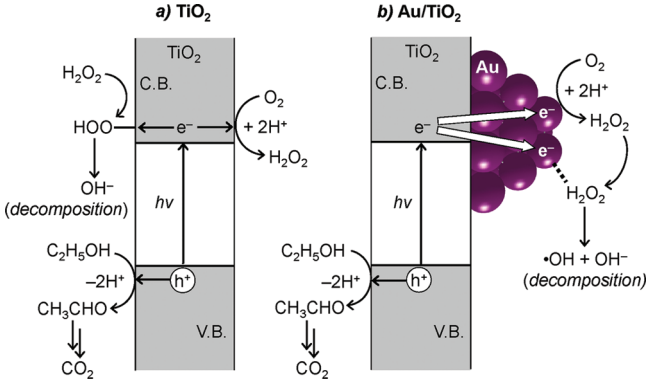

UV irradiation of the catalyst in an O_2-saturated ethanol/water mixture produces H_2O_2 at a millimolar level. As shown in Scheme 1b, the conduction band e^- of TiO_2 is trapped by the Au particles because of the formation of a Schottky barrier at the Au/TiO_2 heterojunction.[13] This suppresses the reduction of Ti–OOH species (H_2O_2 decomposition). In addition, two-electron reduction of O_2 is selectively promoted on the Au particles. These effects enable efficient H_2O_2 production. H_2O_2 molecules are, however, strongly adsorbed onto Au particles[14] and decomposed by the reduction with e^- ($H_2O_2 + e^- \rightarrow$ •OH + OH^-).[15]

Received: December 26, 2011
Revised: February 9, 2012
Published: March 8, 2012

   dx.doi.org/10.1021/cs2006873 | ACS Catal. 2012, 2, 599–603

This means that Au particles promote the formation and decomposition of H_2O_2 simultaneously. Further improvement of H_2O_2 production therefore requires the promotion of H_2O_2 formation while suppressing its decomposition.

Here we report that TiO_2 loaded with Au–Ag bimetallic alloy particles (AuAg/TiO_2) addresses this dilemma and successfully produces H_2O_2. This is achieved via the double effects created by the alloy particles. One is the efficient photocatalytic reduction of O_2 on the Au atoms promoting enhanced H_2O_2 formation, because of the efficient e^-–h^+ separation at the alloy/TiO_2 junction. Second is the suppressed decomposition of H_2O_2 because of the decreased adsorption of H_2O_2 onto the Au atoms.

The $Au_{0.1}Ag_y/TiO_2$ catalysts with alloy particles consisting of 0.1 mol % Au (= Au/TiO_2 × 100) and different amount of Ag [y (mol %) = Ag/TiO_2 × 100] were prepared with Japan Reference Catalyst JRC-TIO-4 TiO_2 particles (similar to Degussa P25; anatase/rutile = ca. 80/20; average particle size, 24 nm) by simultaneous impregnation of $HAuCl_4$ and $AgNO_3$ followed by reduction with H_2 (see Experimental Methods).[16] As shown in Figure 1, a high-resolution transmission electron microscopy (HRTEM) image of $Au_{0.1}Ag_{0.4}/TiO_2$ showed spherical metal particles with average diameter 13.8 nm. An energy dispersive X-ray spectroscopy (EDX) of metal particles on the catalyst (Figure S1, Supporting Information) determined the average Au/Ag ratio as 0.27 (mol/mol). An X-ray photoelectron spectroscopy (XPS) of the catalyst determined the Au/Ag ratio on the surface of metal particles[17] as 0.25 (Figure S2, Supporting Information). These Au/Ag ratios are similar to the ratio of total amounts of Au and Ag (0.26) in the catalyst determined by inductively coupled argon plasma atomic emission spectrometer (ICAP-AES). Diffuse reflectance UV–vis spectra of $Au_{0.1}Ag_y/TiO_2$ (Figure S3, Supporting Information) showed single absorption bands at 519–549 nm, located between the localized surface plasmon resonance for monometallic Au (569 nm) and Ag particles (473 nm).[18,19] These data suggest that the Au and Ag components in the metal particles are mixed homogeneously.

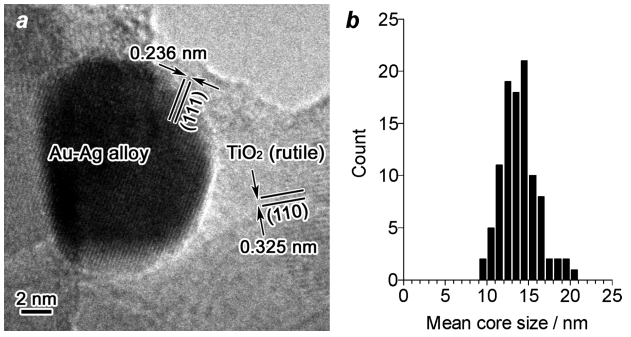

Figure 1. (a) Typical HRTEM image of $Au_{0.1}Ag_{0.4}/TiO_2$ and (b) size distribution of metal particles.

Table 1 summarizes the H_2O_2 concentration in solution after photoirradiation for 12 h at λ >280 nm[20] of water (5 mL) containing 4% ethanol with catalysts (5 mg) at 298 K under 1 atm O_2. With pure TiO_2 (entry 1), the H_2O_2 concentration is only 0.5 mM. In contrast, $Au_{0.1}/TiO_2$ produces larger amount of H_2O_2 (1.2 mM, entry 2), indicating that Au loading indeed enhances H_2O_2 production.[12] Further Au loadings (0.2–0.5 mol %, entries 3–6) show similar H_2O_2 concentrations (~1.5 mM). In contrast, the $Au_{0.1}Ag_y/TiO_2$ alloy catalysts (entries 7–11) produce larger amount of H_2O_2; the increase in Ag amount in the alloy enhances H_2O_2 production, although ≥0.6 mol % Ag loading decreases the activity. Among them, $Au_{0.1}Ag_{0.4}/TiO_2$ (entry 9) produces the largest amount of H_2O_2 (3.4 mM), which is more than double that obtained with Au/TiO_2 (~1.5 mM). As shown in entry 12, TiO_2 loaded with Ag solely ($Ag_{0.4}/TiO_2$) produces only 1.0 mM H_2O_2. The loading of Pt, Pd, or their alloys (Au–Pt or Au–Pd) is also

Table 1. Results of Photocatalytic Production of H_2O_2 on Various Catalysts and the Kinetic Parameters[a]

entry	catalyst	metal particle size/nm[b]	H_2O_2/mM[c]	CH_3CHO/μmol	CO_2/μmol	k_f/(mM h^{-1})[d]	k_d/(h^{-1})[d]
1[e]	TiO_2		0.5	144	11	0.18	0.34
2[e]	$Au_{0.1}/TiO_2$	9.1	1.2	177	17	0.32	0.26
3	$Au_{0.2}/TiO_2$		1.5	189	23	0.44	0.28
4	$Au_{0.3}/TiO_2$		1.5	200	21	0.51	0.33
5	$Au_{0.4}/TiO_2$		1.5	215	37	0.52	0.33
6	$Au_{0.5}/TiO_2$	10.9	1.4	224	42	0.53	0.35
7	$Au_{0.1}Ag_{0.1}/TiO_2$		1.7	190	33	0.42	0.22
8	$Au_{0.1}Ag_{0.2}/TiO_2$		2.3	218	42	0.47	0.18
9[e]	$Au_{0.1}Ag_{0.4}/TiO_2$	13.8	3.4	266	53	0.57	0.14
10	$Au_{0.1}Ag_{0.6}/TiO_2$		1.8	210	36	0.32	0.13
11	$Au_{0.1}Ag_{0.8}/TiO_2$	20.7	1.1	166	13	0.16	0.11
12	$Ag_{0.4}/TiO_2$	8.9	1.0	147	15	0.15	0.12
13	$Pt_{0.4}/TiO_2$		0.8	266	42	0.32	0.39
14	$Pd_{0.4}/TiO_2$		0.7	372	56	0.24	0.34
15	$Au_{0.1}Pt_{0.4}/TiO_2$		1.1	316	56	0.39	0.35
16	$Au_{0.1}Pd_{0.4}/TiO_2$		1.3	407	70	0.45	0.33
17	$Ag_{0.4}$ + $Au_{0.1}/TiO_2$		1.6	187	19	0.32	0.18
18[f]	$Au_{0.1}Ag_{0.4}/TiO_2$		3.6	271	55		
19[g]	$Au_{0.1}Ag_{0.4}/TiO_2$		3.4	267	51		

[a]Reaction conditions: ethanol/water (4/96 v/v) mixture (5 mL), catalyst (5 mg), O_2 (1 atm), temperature (298 K), λ >280 nm, time (12 h). [b]Determined by TEM observations (Figure S4, Supporting Information). [c]Determined by redox titration with $KMnO_4$ (detection limit: 0.05 mM). [d]Determined from the time-dependent change in H_2O_2 concentration using the equation: $[H_2O_2] = (k_f/k_d)\{1 - \exp(-k_d t)\}$ (Figure S5, Supporting Information). The errors for k_f and k_d values are ±0.03 mM h^{-1} and ±0.02 h^{-1}, respectively. [e]Amounts of acetic acid formed were 58 μmol (entry 1), 66 μmol (entry 2), and 82 μmol (entry 9), respectively, where other photooxidation products of ethanol such as methanol and formaldehyde (ref 21) were not detected by GC analysis. [f]First reuse after washing with water. [g]Second reuse.

dx.doi.org/10.1021/cs2006873 | ACS Catal. 2012, 2, 599–603

ineffective (~1.3 mM; entries 13–16). These data indicate that the combination of Au and Ag is important for efficient H_2O_2 production.

As shown in entry 17, the $Ag_{0.4}$ + $Au_{0.1}/TiO_2$ catalyst, prepared by a step-by-step deposition of respective Ag and Au metals onto TiO_2 by repeated impregnation/reduction sequence (see Experimental Methods), produces much lower amount of H_2O_2 (1.6 mM) than $Au_{0.1}Ag_{0.4}/TiO_2$ (3.4 mM, entry 9). This indicates that homogeneously mixed Au–Ag alloy is necessary. Note that the $Au_{0.1}Ag_{0.4}/TiO_2$ catalyst is reusable without loss of activity and selectivity. The catalyst, when reused for further reaction (entries 18 and 19), produces similar amounts of H_2O_2 to that obtained with the virgin catalyst (entry 9).

Figure 2 shows the change in H_2O_2 concentration with time. The rate for H_2O_2 production becomes lower as the time

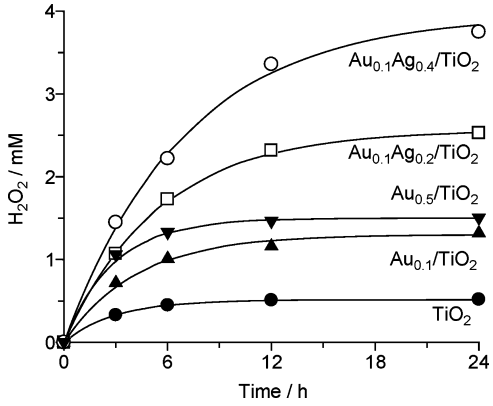

Figure 2. Time-dependent change in H_2O_2 concentration during photoreaction with respective catalysts. The reaction conditions are identical to those in Table 1. The lines are the calculated results using the equation; $[H_2O_2] = (k_f/k_d)\{1 - \exp(1-k_d t)\}$.

advances because of the photocatalytic decomposition of H_2O_2.[9−12] The rates for formation and decomposition of H_2O_2 follow the zero- and first-order kinetics toward H_2O_2 concentration, respectively.[12] The kinetic data are therefore explained by the equation: $[H_2O_2] = (k_f/k_d)\{1 - \exp(-k_d t)\}$, where k_f (mM h^{-1}) and k_d (h^{-1}) are the rate constants for formation and decomposition of H_2O_2, respectively. The rate constants obtained in the respective systems are summarized in Table 1. Au/TiO_2 catalysts show k_f values larger than that of TiO_2 (0.18), and the values increase with the Au loadings (~0.53). This suggests that Au loading is indeed effective for H_2O_2 formation. $Au_{0.1}/TiO_2$ shows k_d value (0.26) lower than that of TiO_2 (0.34), but further Au loading increases the values (~0.35), which are comparable to that of TiO_2. These data indicate that Au particles promote both formation and decomposition of H_2O_2. In contrast, the alloy catalysts show different properties. The k_f value of $Au_{0.1}Ag_{0.4}/TiO_2$ (0.57) is comparable to that of $Au_{0.5}/TiO_2$ (0.53), but its k_d value (0.14) is much lower than that of $Au_{0.5}/TiO_2$ (0.35). These data clearly indicate that high H_2O_2 production efficiency of $Au_{0.1}Ag_{0.4}/TiO_2$ is because the catalyst promotes efficient formation of H_2O_2 while suppressing its decomposition.

As shown in Table 1 (entry 12), $Ag_{0.4}/TiO_2$ is ineffective for H_2O_2 production: it shows a small k_f value (0.15) similar to that of pure TiO_2 (entry 1). The amounts of formed acetaldehyde and CO_2, which are the major photooxidation products of ethanol,[21] show similar tendency (Table 1). This suggests that rapid e^-–h^+ recombination on $Ag_{0.4}/TiO_2$ leads to low photocatalytic activity. As shown in Figure 3b, the Schottky barrier

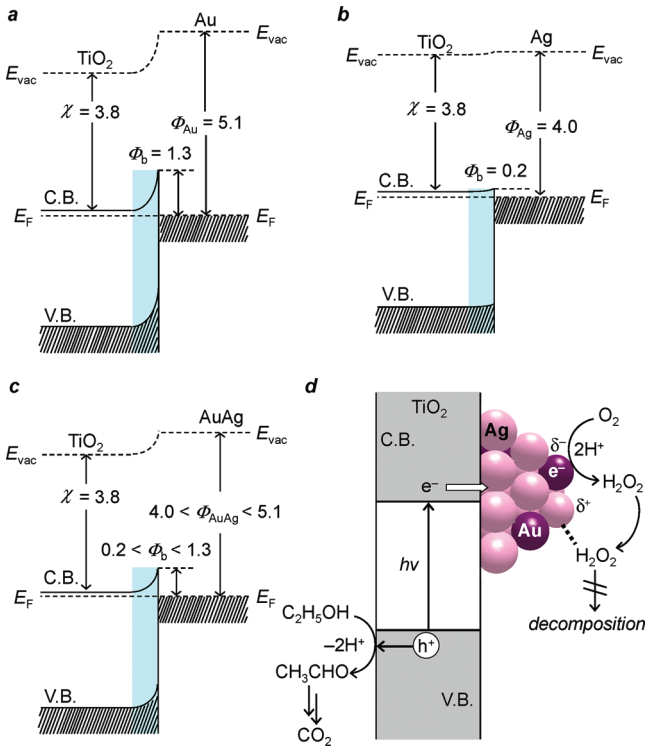

Figure 3. Schematic energy-band diagrams for (a) Au/TiO_2, (b) Ag/TiO_2, and (c) $AuAg/TiO_2$ heterojunction. E_{vac}, E_F, Φ_M, Φ_b, and χ denote vacuum level, Fermi level, work function of metal, Schottky barrier height, and electron affinity of TiO_2 conduction band, respectively (in eV). (d) Mechanism for photocatalytic production of H_2O_2 on $AuAg/TiO_2$ catalyst.

height at the Ag/TiO_2 junction is determined to be only about 0.2 eV,[13] based on the difference between the work function (Φ) of Ag (4.0 eV)[22] and the electron affinity (χ) of TiO_2 conduction band (3.8 eV).[23] This thus results in rapid e^-–h^+ recombination on Ag/TiO_2.[13] In contrast, the Schottky barrier height at the Au/TiO_2 junction (Figure 3a) is much larger (1.3 eV) because of the larger work function of Au (5.1 eV).[22] This enhances e^-–h^+ separation and shows high photocatalytic activity, although larger barrier height suppresses e^- transfer from TiO_2 to Au.[24] The $Au_{0.1}Ag_{0.4}/TiO_2$ alloy catalyst shows photocatalytic activity comparable to $Au_{0.5}/TiO_2$. This is explained by appropriate height of Schottky barrier (Figure 3c). The work function of the alloy lies at the level intermediate between the monometallic Au and Ag.[25] The $alloy/TiO_2$ junction therefore creates a barrier that is larger than Ag/TiO_2 but smaller than Au/TiO_2. This may allow efficient e^-–h^+ separation while promoting smooth e^- transfer from TiO_2 to alloy. Au is more electronegative than Ag; therefore, their alloying leads to an electron donation from Ag to Au.[26] As a result of this, electron density of Au atoms increases,[27] and they promote efficient two-electron reduction of O_2, as shown in Figure 3d. These alloying effects result in high activity for H_2O_2 formation on the $AuAg/TiO_2$ catalyst.

As shown in Table 1 (entries 9–11), $Au_{0.1}Ag_y/TiO_2$ catalysts with ≥0.6 mol % Ag produce lower amounts of H_2O_2 than $Au_{0.1}Ag_{0.4}/TiO_2$; the H_2O_2 amount formed with $Au_{0.1}Ag_{0.8}/TiO_2$ (entry 11) is comparable to that with $Ag_{0.4}/TiO_2$ (entry 12).

dx.doi.org/10.1021/cs2006873 | ACS Catal. 2012, 2, 599–603

This is because the increase in Ag amount of the alloy particles decreases the Schottky barrier height and results in inefficient e^-–h^+ separation. In addition, as shown in Table 1 (entry 17), the $Ag_{0.4}$ + $Au_{0.1}/TiO_2$ catalyst, prepared by a step-by-step deposition of respective Ag and Au metals, produces a much lower amount of H_2O_2 than $Au_{0.1}Ag_{0.4}/TiO_2$. This is probably because incomplete mixing of two metal components leads to insufficient band alignment and does not promote efficient e^-–h^+ separation. These data suggest that the alloy particles with appropriate amounts of Au and Ag that are mixed homogeneously are necessary for efficient H_2O_2 formation.

Another important property of the alloy catalyst is the decreased photocatalytic decomposition of formed H_2O_2. This is because the adsorption of H_2O_2 onto the Au atoms is suppressed because of the increased electron density of Au atoms by the Ag alloying. This is confirmed by ab initio calculation of cubic Au_9, Au_1Ag_8, and Ag_9 clusters that are often used to clarify the electronic properties and catalytic activities of metal nanoparticles with 2–10 nm diameter.[28−31] Figure 4a–c shows the optimized structure of clusters and the Mulliken charge of selected atoms, calculated based on the density functional theory within the Gaussian 03 program. As shown in Figure 4a, the edge Au atoms of the Au_9 cluster are positively charged (0.103). Also in the Ag_9 cluster (Figure 4c), the edge Ag atoms are charged positively (0.056). In contrast, in the Au_1Ag_8 alloy cluster (Figure 4b), the edge Au atom is negatively charged (−0.431), whereas adjacent Ag atoms become more positive. This is due to the electron donation from Ag to Au because of the higher electronegativity of Au.[26] This suggests that the Ag alloying indeed increases the negative charge of Au atoms (Figure 3d).

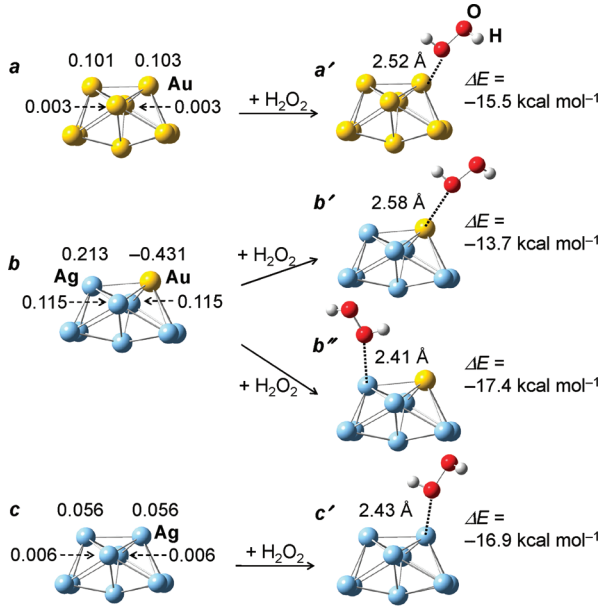

Figure 4. Optimized structures and Mulliken charges of (a) Au_9, (b) Au_1Ag_8, and (c) Ag_9 clusters, and (a′, b′, b″, c′) the distances and adsorption energies for metal···H_2O_2 interaction, calculated by B3LYP/6-31+G/LANL2DZ basis set.

The adsorption energies between H_2O_2 and respective metal atoms were then calculated.[32] As shown in Figure 4a′ and b′, the adsorption energy between H_2O_2 and the Au atom on the Au_1Ag_8 alloy (−13.7 kcal mol^{-1}) is more positive than that on Au_9 (−15.5 kcal mol^{-1}). This indicates that the affinity between H_2O_2 and Au is decreased by the Ag alloying because of the increased negative charge of Au. In contrast, as shown in Figure 4b″, the adsorption energy between H_2O_2 and the Ag atom in the alloy is more negative (−17.4 kcal mol^{-1}). This suggests that, on the alloy particle, H_2O_2 is preferably adsorbed onto the Ag atoms. The photocatalytic reduction by e^- on the alloy occurs mainly on the negatively charged Au, as shown in Figure 3d; therefore, the positively charged Ag is inactive for reduction of H_2O_2 adsorbed. These suggest that decreased adsorption of H_2O_2 onto the Au atoms suppresses the photocatalytic decomposition of H_2O_2.

In summary, we found that TiO_2 photocatalyst loaded with Au–Ag alloy particles promotes efficient H_2O_2 production by the double effects of alloy particles: (i) the efficient e^-–h^+ separation at the alloy/TiO_2 junction, promoting efficient H_2O_2 formation; and, (ii) decreased H_2O_2 adsorption onto the Au atoms, suppressing decomposition of formed H_2O_2. The efficiency for H_2O_2 production by this method is much lower than those of the conventional anthraquinone method and the direct synthesis method with H_2 and O_2. Nevertheless, the concept proposed here with alloy particles may contribute to the design of more efficient photocatalytic H_2O_2 production. So far, some photocatalysts loaded with alloy particles have been proposed; however, there are only two reports of selective organic transformations.[16,33] The successful example presented here, which promotes efficient formation of targeted product while suppressing subsequent reaction of product by the alloying effects, may open a new strategy toward the development of new alloy photocatalysts and contribute to the design of photocatalytic systems for selective organic transformations.

EXPERIMENTAL METHODS

Preparation of $Au_{0.1}Ag_y/TiO_2$. TiO_2 (1.0 g) was added to water (50 mL) containing $HAuCl_4{\cdot}4H_2O$ (5.6 mg) and $AgNO_3$ (1.6, 3.9, 7.9, 11.9, or 15.9 mg). The pH of solution was adjusted to about 7 with a NaOH solution (1 mM),[34] and water was evaporated at 353 K with stirring. The powders were dried in vacuo at 353 K for 12 h, calcined in air at 673 K for 2 h, and reduced with H_2 at 773 K for 1 h, affording $Au_{0.1}Ag_y/TiO_2$ (y = 0.1, 0.2, 0.4, 0.6, 0.8). $Ag_{0.4}/TiO_2$, $Pt_{0.4}/TiO_2$, $Pd_{0.4}/TiO_2$, $Au_{0.1}Pt_{0.4}/TiO_2$, and $Au_{0.1}Pd_{0.4}/TiO_2$ catalysts were prepared in a similar manner using $AgNO_3$, H_2PtCl_6, and $PdCl_2$ as metal precursors.

Preparation of Au_x/TiO_2. TiO_2 (1.0 g) was added to water (50 mL) containing $HAuCl_4{\cdot}4H_2O$ (5.6, 11.3, 16.9, 22.9, or 28.4 mg). The pH of solution was adjusted to about 7, and the solution was stirred at 353 K for 3 h. The powders were recovered by centrifugation, washed with water, and dried in vacuo at 353 K for 12 h. The obtained powders were calcined under air at 773 K for 4 h, affording Au_x/TiO_2 (x = 0.1, 0.2, 0.3, 0.4, 0.5).

Preparation of $Ag_{0.4}$ + $Au_{0.1}/TiO_2$. TiO_2 (1.0 g) was added to water (50 mL) containing $AgNO_3$ (7.9 mg). The pH of solution was adjusted to about 7, and water was evaporated at 353 K. The powders were dried in vacuo at 353 K for 12 h, calcined under air at 673 K for 2 h, and reduced with H_2 at 773 K for 1 h. The obtained powders were added to water (50 mL) containing $HAuCl_4{\cdot}4H_2O$ (5.6 mg). The pH of solution was adjusted to about 7, and water was evaporated at 353 K. The resulting powders were dried in vacuo at 353 K for 12 h, calcined under air at 673 K for 2 h, and reduced with H_2 at 773 K for 1 h.

dx.doi.org/10.1021/cs2006873 | ACS Catal. 2012, 2, 599–603

Photoreaction Procedure. Catalyst (5 mg) was suspended in an ethanol/water mixture (4/96 v/v; 5 mL) within a Pyrex glass tube (φ10 mm; capacity, 20 mL), and the tube was sealed with a rubber septum cap. After ultrasonication (5 min) and O_2 bubbling (5 min), the solution was photoirradiated (λ >280 nm) with magnetic stirring by a 450 W high pressure Hg lamp (USHIO Inc.). The light intensity at 280−400 nm was 13.8 mW cm^{-2}. The temperature of solution was kept at 298 ± 0.5 K with a temperature-controlled water bath. The gas-phase product was analyzed by GC-TCD (Shimadzu; GC-14B). The catalyst was recovered by centrifugation, and the liquid-phase product was analyzed by GC-FID. The H_2O_2 concentration in solution was determined by the redox titration with $KMnO_4$.

Analysis. Total amounts of Au and Ag in catalysts were determined by an ICAP-AES (SII Nanotechnology; SPS 7800) after dissolution in aqua regia or nitric acid. TEM observations were performed using an FEI Tecnai G2 20ST analytical electron microscope operated at 200 kV, which is equipped with an EDX spectroscopy detector. The spectra were taken under Scanning TEM mode. XPS analysis was carried out using a JEOL JPS-9000MX spectrometer using Mg Kα radiation as the energy source. Diffuse reflectance UV−vis spectra were measured on an UV−vis spectrophotometer (Jasco Corp.; V-550 with Integrated Sphere Apparatus ISV-469) with $BaSO_4$ as a reference.

Calculation Details. Calculations were performed using the DFT theory within the Gaussian 03 program. Geometry optimizations were carried out at the B3LYP/6-31+G level for H and O atoms and at the B3LYP/LANL2DZ level for Au and Ag. Adsorption energies (ΔE) between H_2O_2 and metal clusters were determined with the equation: $\Delta E = E$ (metal cluster···H_2O_2) − [E (metal cluster) + E (H_2O_2)]. The total energies, Cartesian coordinates, and Mulliken charges for all atoms are summarized at the end of the Supporting Information.

■ ASSOCIATED CONTENT

Supporting Information

EDX spectra (Figure S1), XPS results (Figure S2), diffuse-reflectance spectra (Figure S3), TEM images and the size distribution of metal particles (Figure S4), time-dependent change in H_2O_2 concentration (Figure S5), and calculation results. This material is available free of charge via the Internet at http://pubs.acs.org.

■ AUTHOR INFORMATION

Corresponding Author

*E-mail: shiraish@cheng.es.osaka-u.ac.jp.

Funding

This work was supported by the Grant-in-Aid for Scientific Research (No. 23360349) from the Ministry of Education, Culture, Sports, Science, and Technology, Japan (MEXT). D.T. thanks the Japan Society for Promotion of Science (JSPS) for Young Scientist.

Notes

The authors declare no competing financial interest.

■ REFERENCES

(1) Campos-Martin, J. M.; Blanco-Brieva, G.; Fierro, J. L. G. *Angew. Chem., Int. Ed.* **2006**, *45*, 6962−6984.
(2) Choudhary, V. R.; Gaikwad, A. G.; Sansare, S. D. *Angew. Chem., Int. Ed.* **2001**, *40*, 1776−1779.
(3) Landon, P.; Collier, P. J.; Papworth, A. J.; Kiely, C. J.; Hutchings, G. J. *Chem. Commun.* **2002**, 2058−2059.
(4) Lunsford, J. H. *J. Catal.* **2003**, *216*, 455−460.
(5) Blanco-Brieva, G.; Cano-Serrano, E.; Campos-Martin, J. M.; Fierro, J. L. *Chem. Commun.* **2004**, 1184−1185.
(6) Melada, S.; Rioda, R.; Menegazzo, F.; Pinna, F.; Strukul, G. *J. Catal.* **2006**, *239*, 422−430.
(7) Edwards, J. K.; Solsona, B.; Ntainjua, N, E.; Carley, A. F.; Herzing, A. A.; Kiely, C. J.; Hutchings, G. J. *Science* **2009**, *323*, 1037−1041.
(8) Gosser, L. W. (E. I. Du Pont de Nemours and Company), Patent EP132294, **1985** [*Chem. Abstr.* **1985**, *102*, 134404].
(9) Kormann, C.; Bahnemann, D. W.; Hoffmann, M. R. *Environ. Sci. Technol.* **1988**, *22*, 798−806.
(10) Li, X.; Chen, C.; Zhao, J. *Langmuir* **2001**, *17*, 4118−4122.
(11) Maurino, V.; Minero, C.; Mariella, G.; Pelizzetti, E. *Chem. Commun.* **2005**, 2627−2629.
(12) Teranishi, M.; Naya, S.; Tada, H. *J. Am. Chem. Soc.* **2010**, *132*, 7850−7851.
(13) Linsebigler, A. L.; Lu, G.; Yates, J. T. Jr. *Chem. Rev.* **1995**, *95*, 735−758.
(14) Miah, M. R.; Ohsaka, T. *Anal. Chem.* **2006**, *78*, 1200−1205.
(15) Hirakawa, T.; Yawata, K.; Nosaka, Y. *Appl. Catal. A: Gen.* **2007**, *325*, 105−111.
(16) Shiraishi, Y.; Takeda, Y.; Sugano, Y.; Ichikawa, S.; Tanaka, S.; Hirai, T. *Chem. Commun.* **2011**, *47*, 7863−7865.
(17) Edwards, J. K.; Solsona, B. E.; Landon, P.; Carley, A. F.; Herzing, A.; Kiely, C. J.; Hutchings, G. J. *J. Catal.* **2005**, *236*, 69−79.
(18) Chiarello, G. L.; Aguirre, M. A.; Selli, E. *J. Catal.* **2010**, *273*, 182−190.
(19) Smetana, A. B.; Klabunde, K. J.; Sorensen, C. M.; Ponce, A. A.; Mwale, B. *J. Phys. Chem. B* **2006**, *110*, 2155−2158.
(20) The reaction scarcely occurs under irradiation of visible light (λ > 420 nm): <0.1 mM H_2O_2, 3 μmol of acetaldehyde, and 0.3 μmol of CO_2 are produced even after 12 h of photoirradiation, indicating that the photoexcitation of TiO_2 initiates the H_2O_2 production.
(21) Hirakawa, T.; Koga, C.; Negishi, N.; Takeuchi, K.; Matsuzawa, S. *Appl. Catal. B: Environ.* **2009**, *87*, 46−55.
(22) Eastman, D. *Phys. Rev. B* **1970**, *2*, 1−2.
(23) Tokmoldin, N.; Griffiths, N.; Bradley, D. D. C.; Haque, S. A. *Adv. Mater.* **2009**, *21*, 3475−3478.
(24) Uchihara, T.; Matsumura, M.; Yamamoto, A.; Tsubomura, H. *J. Phys. Chem.* **1989**, *93*, 5870−5874.
(25) Gong, H. R. *Mater. Chem. Phys.* **2010**, *123*, 326−330.
(26) Pande, S.; Ghosh, S. K.; Praharaj, S.; Panigrahi, S.; Basu, S.; Jana, S.; Pal, A.; Tsukuda, T.; Pal, T. *J. Phys. Chem. C* **2007**, *111*, 10806−10813.
(27) Taufany, F.; Pan, C.-J.; Chou, H.-L.; Rick, J.; Chen, Y.-S.; Liu, D.-G.; Lee, J.-F.; Tang, M.-T.; Hwang, B.-J. *Chem.—Eur. J.* **2011**, *17*, 10724−10735.
(28) Li, Z.; Ciobanu, C. V.; Hu, J.; Palomares-Báez, J.-P.; Rodríguez-López, J.-L.; Richards, R. *Phys. Chem. Chem. Phys.* **2011**, *13*, 2582−2589.
(29) Barnglover, B. M.; Aikens, C. M. *J. Phys. Chem. A* **2011**, *115*, 11818−11823.
(30) Lopez, N.; Nørskov, J. K. *J. Am. Chem. Soc.* **2002**, *124*, 11262−11263.
(31) Kiyonaga, T.; Mitsui, T.; Soejima, T.; Ito, S.; Tada, H.; Kawahara, T.; Akita, T.; Tanaka, K.; Kobayashi, H. *ChemPhysChem* **2005**, *6*, 2508−2512.
(32) Balbuena, P. B.; Calvo, S. R.; Lamas, E. J.; Salazar, P. F.; Seminario, J. M. *J. Phys. Chem. B* **2006**, *110*, 17452−17459.
(33) Yamauchi, M.; Abe, R.; Tsukuda, T.; Kato, K.; Takata, M. *J. Am. Chem. Soc.* **2011**, *133*, 1150−1152.
(34) ICAP-AES analysis suggested that the $Au_{0.1}Ag_{0.4}/TiO_2$ catalyst contains about 0.25 wt % Na. To clarify the effect of Na on the photocatalytic activity, we prepared the catalyst with 1 M NH_3 instead of 1 M NaOH. Photoreaction (12 h) with the obtained catalyst produces H_2O_2 (3.1 mM), acetaldehyde (221 μmol), acetic acid (81 μmol), CO_2 (47 μmol). These data are similar to that of the catalyst prepared with NaOH (Table 1, entry 9). This suggests that Na contained in the catalyst scarcely affects the photocatalytic activity.